© 2014. Published by The Company of Biologists Ltd | The Journal of Experimental Biology (2014) 217, 1737-1744 doi:10.1242/jeb.098665

RESEARCH ARTICLE

Octopaminergic modulation of the visual flight speed regulator of *Drosophila*

Floris van Breugel[1,*], Marie P. Suver[2] and Michael H. Dickinson[2]

ABSTRACT

Recent evidence suggests that flies' sensitivity to large-field optic flow is increased by the release of octopamine during flight. This increase in gain presumably enhances visually mediated behaviors such as the active regulation of forward speed, a process that involves the comparison of a vision-based estimate of velocity with an internal set point. To determine where in the neural circuit this comparison is made, we selectively silenced the octopamine neurons in the fruit fly *Drosophila*, and examined the effect on vision-based velocity regulation in free-flying flies. We found that flies with inactivated octopamine neurons accelerated more slowly in response to visual motion than control flies, but maintained nearly the same baseline flight speed. Our results are parsimonious with a circuit architecture in which the internal control signal is injected into the visual motion pathway upstream of the interneuron network that estimates groundspeed.

KEY WORDS: Octopamine, *Drosophila*, Flight control

INTRODUCTION

Many animals modulate the properties of their neural networks according to behavioral state in order to increase their functionality (Marder and Bucher, 2007), a principle that presumably applies to control circuits that regulate behavioral actions. Studies in mice (Andermann et al., 2011; Niell and Stryker, 2010), monkeys (Moran and Desimone, 1985; Treue and Maunsell, 1996) and flies (Jung et al., 2011; Maimon et al., 2010) show that modulation of the visual processing system in particular is a common feature across taxa; however, the behavioral implications of these modulations are unknown. Increasing the sensitivity of the visual system during certain behaviors might allow these animals to react more quickly to visual disturbances through a sensory-motor feedback control loop.

Feedback control works by comparing a perceived sensory signal with a desired output, and adjusting motor actions to minimize their difference. Within such a circuit, there are two fundamentally different locations where modulation (e.g. changes in gain) might take place: in the sensory system (before the comparison is made), or in the controller (after the comparison is made). Our current understanding of the underlying neuroanatomy in monkeys, mice and flies would suggest that this gain modulation is situated on the sensory side of the feedback comparison (Fig. 1, H1). However, gain changes in sensory signals can lead to unpredictable behavioral responses because of a large bias introduced to the error signal when the desired value is not equal to zero (Fig. 1, H1). One solution would be to link changes in sensory gain with simultaneous and identical changes in the branch including the command input, so that the error signal is balanced (Fig. 1, H2a). Mismatched changes in the two branches, however, would also result in unpredictable behaviors (Fig. 1, H2a, blue trace).

A simpler alternative is to modulate the gain of the feedback controller that operates on the error signal (Fig. 1, H2b). To incorporate this approach for a visual-motor task would necessitate that an animals' desired reference signal enters the visual stream early, upstream of the neuromodulatory inputs that alter sensory gain. Although topologically distinct, H2a and H2b are mathematically identical if the gain modulations in the two branches of H2a are identical: H2a control input=(gain)(set point)–(gain)(sensory feedback), and H2b control input=(gain)(set point–sensory feedback).

Designing neurobiological experiments that can distinguish between H1 and H2 requires the ability to artificially modulate a specific neural circuit involved in a well-characterized feedback control task without affecting other aspects of behavior. The fruit fly *Drosophila melanogaster* is particularly well suited for addressing this question, because genetic tools make it possible to selectively label and manipulate the activity of small groups of neurons in intact behaving animals (Ofstad et al., 2011; Simpson, 2009; Venken et al., 2011).

In flies and other species of insects, estimates of self-motion are extracted from patterns of optic flow. Local optic flow is estimated by a two-dimensional array of so-called elementary motion detectors (Borst et al., 2010; Brinkworth and O'Carroll, 2009; Egelhaaf et al., 1989; Hassenstein and Reichardt, 1956) and then integrated across visual space by large interneurons in the lobula plate. The lobula plate tangential cells (LPTCs) are particularly well characterized and many exhibit receptive fields that make them sensitive to different patterns of self-motion, such as those created by rotation and translation during flight (Karmeier et al., 2006; Kern et al., 2005; Krapp and Hengstenberg, 1996). This LPTC network is thought to serve a crucial role in flight control, a hypothesis supported by the connections between LPTCs and descending pathways controlling wing and neck motor neurons (Gronenberg and Strausfeld, 1990; Strausfeld and Bassemir, 1985; Strausfeld and Seyan, 1985). Additional experiments in which lobula plate neurons are ablated (Geiger and Nässel, 1981; Hausen and Wehrhahn, 1983; Heisenberg et al., 1978) or activated (Haikala et al., 2013) by physical or genetic means add further support to this hypothesis.

Recent studies in *Drosophila* suggest that gain modulation of the LPTC network occurs during both walking (Chiappe et al., 2010) and flight (Maimon et al., 2010). In the case of flight, this modulation appears to be mediated by octopamine neurons that become active during flight and cause an increase in the gain of the visual responses in at least one class of LPTCs, the vertical system (VS) cells (Suver et al., 2012). Evidence from other flies (Jung et al., 2011; Longden and Krapp, 2010) suggests that gain modulation

[1]California Institute of Technology, Pasadena, CA 91125, USA. [2]Department of Biology, University of Washington, Seattle, WA 35180, USA.

*Author for correspondence (floris@caltech.edu)

Received 18 October 2013; Accepted 29 January 2014

The Journal of Experimental Biology (2014) doi:10.1242/jeb.098665

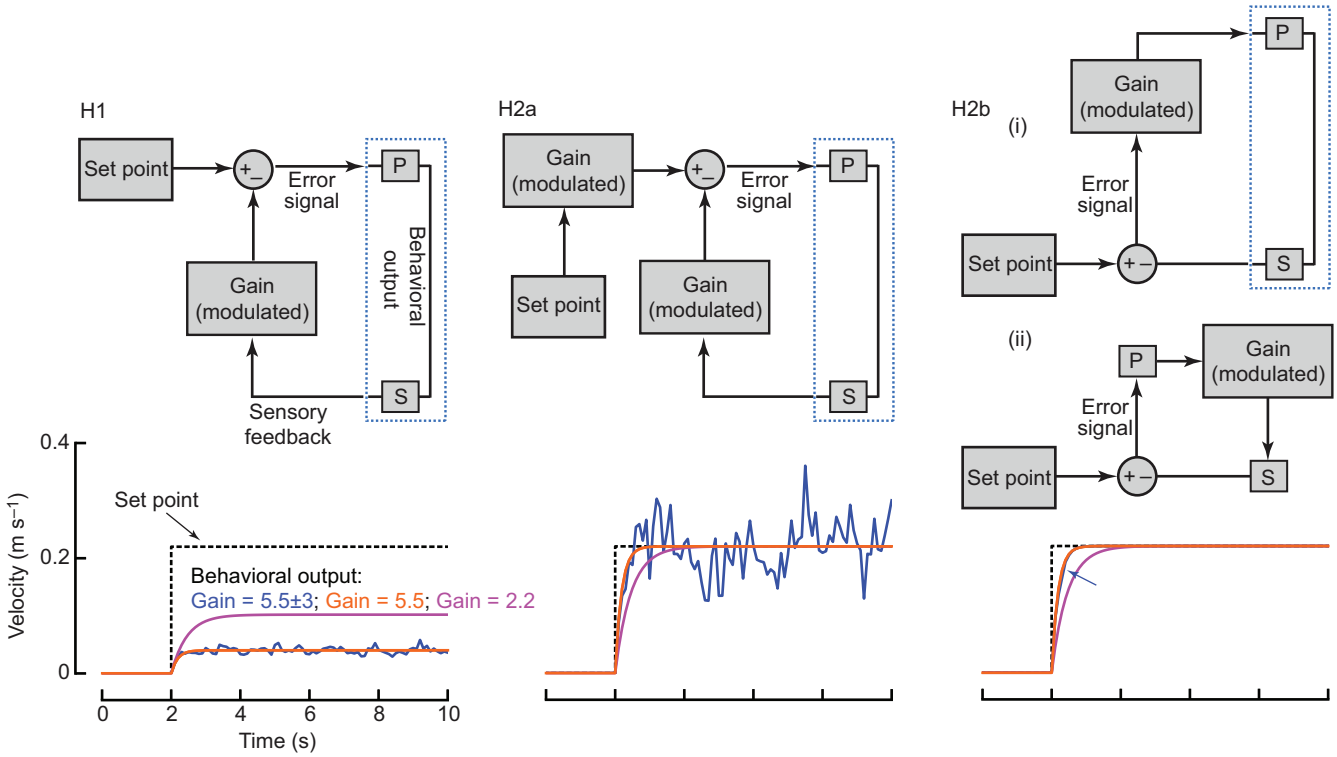

Fig. 1. Feedback control block diagrams, describing the three potential control model architectures under consideration. The portions outlined by the dashed blue lines are identical in each case. P represents the controller dynamics, body dynamics and biomechanics; S represents the sensory perception of the behavioral output (e.g. vision). Below each diagram are the closed-loop responses of the system to a step input of a velocity set point for three different gain settings corresponding to a normally distributed gain of 5.5 with a standard deviation of 3 (blue), a constant gain of 5.5 (orange) and a constant gain of 2.2 (magenta). For these simulations, P operated as a simple integrator, and S was 1. For H2b, we show two architectures that are mathematically identical, yet have different architectural interpretations. In (i), the gain modulation is placed prior to P, a placement that is consistent with the idea that changes in gain occur early in the visual system. In (ii), the gain modulation is placed after P, a placement that is consistent with the idea that changes in gain occur later in the system, such as in downstream motor neurons.

during flight is not restricted to VS cells, but may represent a ubiquitous feature of optic flow processing (Busch et al., 2009). Thus, modulation by octopamine probably increases the sensitivity to many large-field visual cues, perhaps allowing the fly to react more quickly to visual disturbances during flight. In this study, we test this hypothesis directly by observing flies' velocity and acceleration responses to translational visual motion with and without octopamine by genetically silencing their octopamine-producing neurons. Then, we use our results to distinguish between the two models proposed in Fig. 1.

RESULTS

To study the functional role of octopamine-mediated modulation in the visual system, we examined the velocity control system of flies in free flight. Previous studies showed that flies use large-field visual motion to regulate their flight speed about a fixed visual motion set point (Fry et al., 2009; Medici and Fry, 2012). Flies maintain a constant groundspeed over a large range of headwind velocities (David, 1982), demonstrating that this vision-based feedback system is quite robust. Assuming that the LPTC network plays a role in this behavior by estimating the groundspeed from optic flow, then the flies' ability to regulate forward flight speed should be compromised by silencing the octopamine neurons, thereby reducing or eliminating the gain boost in the network during flight. We tested this hypothesis by presenting regressive (back-to-front) visual motion to flying flies and recording their flight trajectories with a 3D tracking system (Fig. 2A; see Materials and methods for additional details). Our visual stimulus consisted of a moving contrast grating (spatial frequency=4.2 m^{-1}) presented at a temporal frequency that varied between trials from 0 to 16 Hz (corresponding to 0–3.8 m s^{-1} linear pattern velocity). To determine the role of octopamine in this behavior, we silenced putative octopaminergic neurons by expressing the inwardly rectifying potassium channel Kir2.1 (Johns et al., 1999) using the *Tdc2-Gal4* driver line (Fig. 2B).

Flies responded to the regressive visual motion by accelerating in the direction of the stimulus after an initial delay of ~100–150 ms (Fig. 3A–C). The magnitude of the acceleration increased monotonically with the temporal frequency of the motion stimulus (Fig. 3). However, for temporal frequencies of 1 Hz (0.23 m s^{-1} linear pattern velocity) and higher, flies with inactivated octopamine neurons (*UAS-Kir2.1/Tdc2-Gal4*) showed significantly lower accelerations when compared with either parental controls (*UAS-Kir2.1/+* and *Tdc2-Gal4/+*), whereas we found no significant differences in acceleration responses exhibited by the two parental controls at any temporal frequency, with the exception of 8 Hz (Fig. 3E). Across all genetic lines, and all temporal frequencies, over 92% of the flies' velocity was in the direction of visual motion for the duration of the trials. Baseline flight speeds were just slightly higher for the flies with inactivated octopamine neurons (*UAS-Kir2.1/Tdc2-Gal4*) (median 0.26 m s^{-1}) compared with parental controls (medians 0.23, 0.21 m s^{-1}; Fig. 3F).

In addition to its role in gain modulation of the visual pathway, octopamine is known to influence a wide range of physiological effects. In our experiments, female flies with Kir2.1 expression in

The Journal of Experimental Biology (2014) doi:10.1242/jeb.098665

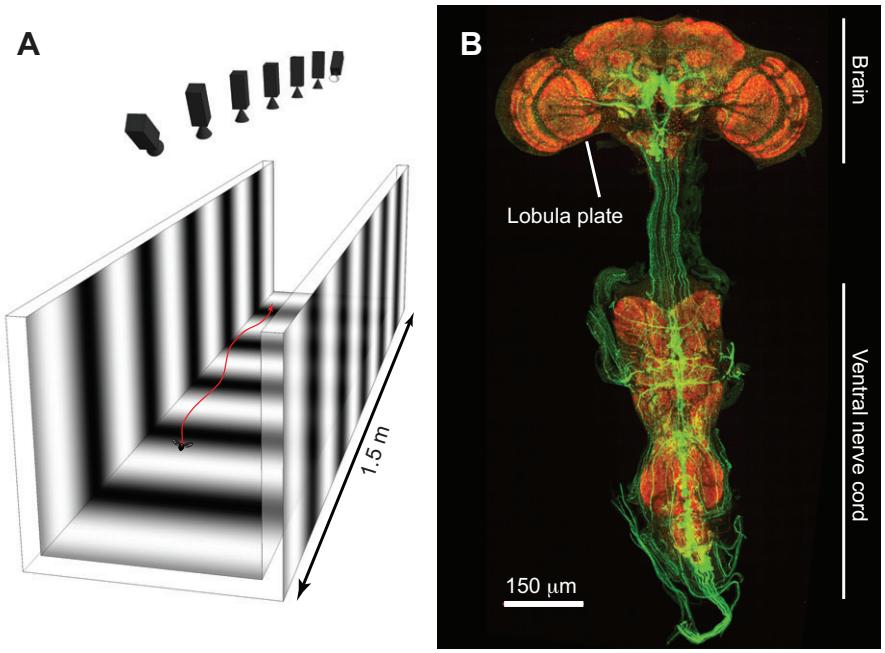

Fig. 2. Free flight arena and genetic expression of octopamine neurons. (A) Tunnel in which the experiments were performed, with a properly scaled representation of the 4.2 m^{-1} spatial frequency used during the experiments. The fly is not to scale. (B) Confocal image of a *Drosophila* brain and ventral nerve cord showing the GFP-labeled octopamine neurons (green), which we genetically silenced with Kir2.1. Red labels neuropil.

their octopamine neurons exhibited a swollen abdomen that is consistent with tonically low octopamine levels and the inability to oviposit (Monastirioti et al., 1996). To test whether our results could be explained by the additional mass of the gravid female flies, we repeated the experiment with males of each genetic line (Fig. 3C). The results for male flies were very similar, indicating that our results for females were not due to differences in abdominal mass.

Octopamine is also known to play a role in body tissues such as muscle (Orchard et al., 1993). Thus, another possibility is that the inhibition of the octopamine system could negatively affect the flies' ability to accelerate via its action on the motor system. The maximum acceleration we observed in the *Tdc2-Gal4/UAS-Kir2.1* flies was 1.5 m s^{-2}, elicited by a temporal frequency of 16 Hz. This magnitude of acceleration would be sufficient to match the accelerations generated by control flies at temporal frequencies of 1–2 Hz. However, even at these low temporal frequencies, the flies with inactivated octopamine neurons accelerated significantly less than the parental controls. Therefore, the absence of octopamine does not fundamentally affect the flies' ability to accelerate. Thus, although we cannot rule out effects on the motor system, we believe that a reduced gain of the large-field visual interneurons provides the most parsimonious explanation for the diminished optomotor performance of the *Tdc2-Gal4/UAS-Kir2.1* flies.

DISCUSSION

To test the models presented in Fig. 1, we constructed a control theoretic model of the flight speed regulator based on, but not identical to, earlier models (Fry et al., 2009; Fuller et al., 2014; Rohrseitz and Fry, 2011) (Fig. 4A). Although the focus of our analysis is on the visual processing and flight control, in order to build a functional model it is necessary to incorporate an accurate prediction of a fly's passive flight dynamics as well. Following the example of Fuller (Fuller et al., 2014), we modeled the passive flight dynamics as a simple unity gain low pass filter with a time constant of 170 ms, which takes into account the aerodynamic drag on a fly's flapping wings as well as inertial effects of its body mass. At high temporal frequencies, the flies exhibited maximum accelerations of up to 2.9 m s^{-2}, which is similar to the maximum of 2.5 m s^{-2} found by Rohrseitz and Fry (Rohrseitz and Fry, 2011). This saturation of the acceleration response presumably represents a biomechanical limit, and we modeled it by incorporating an acceleration saturation, although we present the results both with and without the saturation. Prior experiments have demonstrated that flies exhibit an antenna-mediated reflex that increases the active damping of their flight controller in response to fast changes in air speed (Fuller et al., 2014). Although this component only marginally affects the dynamics in our model, we include it for completeness. The effect of the antenna is nearly identical to the passive flight dynamics, resulting in a unity gain low pass filter with a time constant of 170 ms and a 20 ms delay.

Previous models of the groundspeed regulator have described the visual processing dynamics of the fly as a pure delay (Fuller et al., 2014; Rohrseitz and Fry, 2011). However, this treatment ignores the temporal frequency dependence introduced by early motion processing in the optic lobes, a feature that is thought to emerge from the fundamental properties of motion detectors (Egelhaaf et al., 1989; Hassenstein and Reichardt, 1956). To describe these filter dynamics more completely, we estimated this function based on published electrophysiological recordings of VS cells within the LPTC network (Suver et al., 2012) (Fig. 4B). Although the VS cells are believed to detect rotational motion, rather than forward motion, these behaviors are related because changes in forward velocity are accompanied by changes in pitch (Medici and Fry, 2012). Although data from other cell classes would be helpful, at the moment the VS recordings are the most relevant data available on which we can base our model. The recordings also provide an accurate estimate of the processing delay accrued before the LPTC network (36±12 ms; Fig. 4C). Prior models of groundspeed regulation used a pure delay of 100 ms; to account for this total delay we included a 64 ms delay in the process dynamics. As in previously proposed models of flight speed control (Fuller et al., 2014), we chose an integral type controller, which is necessary to explain a fly's ability to maintain constant flight speed in variable wind conditions (David, 1982).

Although it consists of many components, our dynamic model contains only one free parameter, a proportional gain term, which we chose using MATLAB's implementation of the Nelder–Mead

The Journal of Experimental Biology (2014) doi:10.1242/jeb.098665

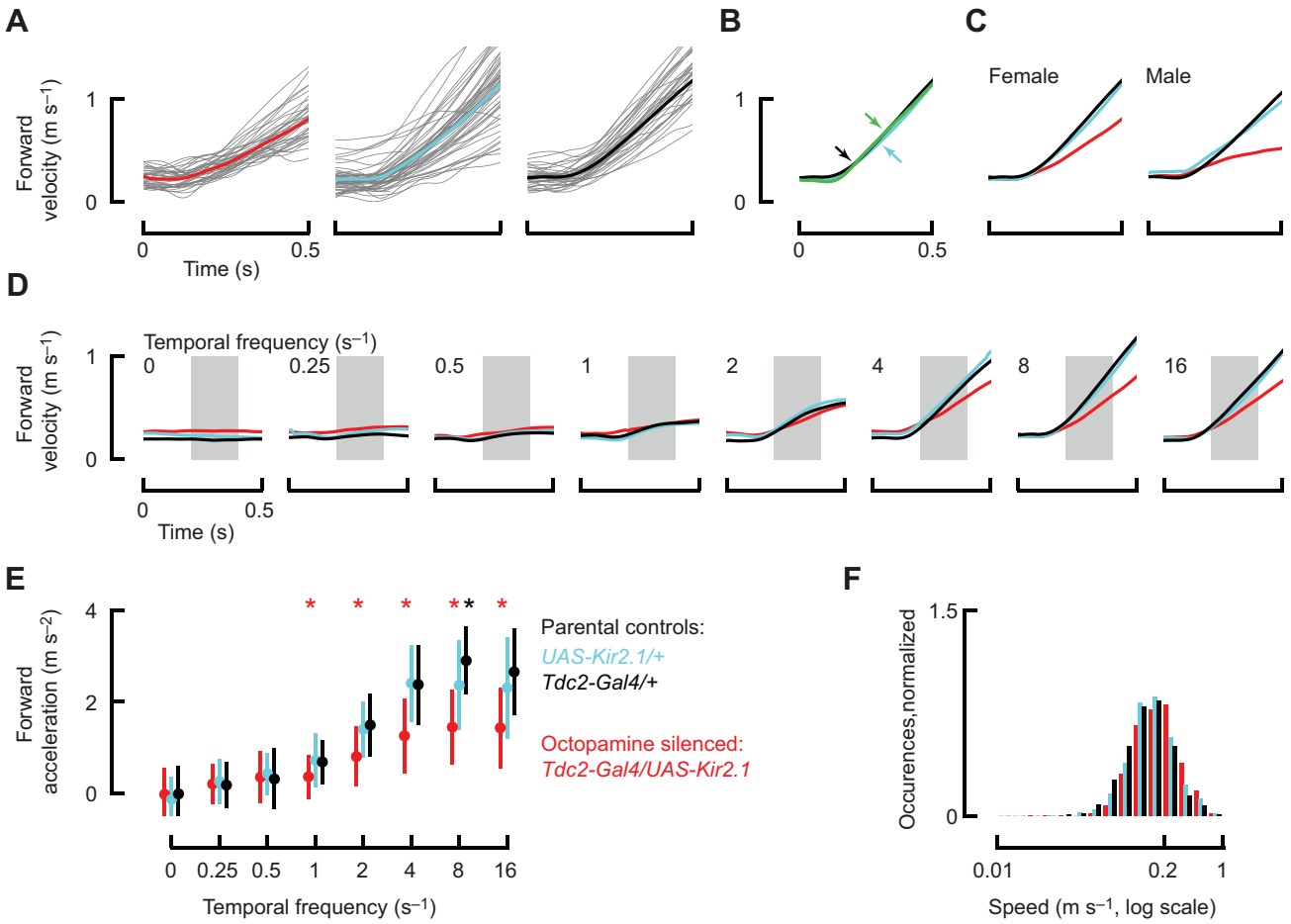

Fig. 3. Octopamine-null flies respond to regressive visual motion during free flight with lower accelerations than wild-type flies. (A) Individual (gray) and mean (colored) velocity versus time responses to regressive visual motion with a temporal frequency of 8 Hz for flies with inactivated octopamine neurons (red), and the parental controls (blue, black). We use consistent colors in subsequent panels. The visual motion started at t=0. (B) Mean velocity responses to an 8 Hz temporal frequency stimulus for the parental controls (blue, black), compared with wild-type flies (green, N=88) (Heisenberg/Canton-S strain). The responses are almost identical; the arrows are included to indicate that each of the three curves is indeed plotted. (C) Mean velocity responses to an 8 Hz temporal frequency stimulus for the parental controls and flies with inactivated octopamine neurons for females and males. (D) Mean velocity responses to regressive motion at different temporal frequencies (for each genotype of each temporal frequency, 42≤N≤106). For the sake of graphical clarity, we chose not show the variance in these traces. The raw traces from A are representative of the data from other temporal frequencies. (E) Acceleration responses to regressive motion versus temporal frequency (mean ± s.d.). Accelerations for each trajectory were calculated as their mean acceleration during the 200–400 ms window after the stimulus was triggered, shown as a gray background in C. Significant differences in acceleration behavior between the flies with inactivated octopamine neurons (red) and the parental controls (blue, black) are indicated for each temporal frequency with red asterisks (P<0.001). A significant difference between the two parental controls is indicated with a black asterisk (P<0.001). (F) Histogram of steady-state velocities for trajectories 1 ms prior to the onset of the regressive motion stimulus.

simplex search method (*fminsearch*) (Lagarias et al., 1998). To account for the differences in visual motion gain between control flies and those with inactivated octopamine neurons, we used this method to choose proportional gain with values of 5.5 and 2.2, respectively. To match the steady-state behavior of the parental controls, we used a preferred visual set point of 0.22 m s^{-1} for the H2 model (which is equivalent to our observed median baseline flight speed), and set point of 1.2 m s^{-1} for the H1 model (which is equivalent to the product of the gain, 5.5, and the observed median baseline flight speed of 0.22 m s^{-1}).

Both models are equally accurate at predicting the observed temporal frequency-dependent acceleration responses, with an octopamine-mediated increase in gain (from 2.2 to 5.5) of 150% during flight (Fig. 4D). The maximum acceleration of the flies with inactivated octopamine neurons lies well below the biomechanical saturation limit of 2.5 m s^{-2}, and their behavior is well captured by the low pass filter derived directly from physiology experiments. The behavior of the parental control lines is best explained by a model that includes a biomechanical saturation. The two models differ substantially, however, in their steady-state predictions (Fig. 4E). According to the H1 model, a reduction in gain due to the absence of octopamine would result in a 150% increase in steady-state flight speed, whereas the H2 model predicts that there would be no change in steady-state flight speed. In our experiments, the flies with inactivated octopamine neurons showed only a marginal increase in flight speed of 18%, despite the fact that these flies accelerated more slowly in response to visual motion than did control flies (Fig. 3A,D). Of these two models, our results are best explained by H2.

H2a is mathematically indistinguishable from H2b because the gain is simply distributed to multiply the preceding blocks (the sensory signal, and the desired set point) independently. The differences between the models do, however, have significant implications for the neural implementation. Any mismatch in the

The Journal of Experimental Biology (2014) doi:10.1242/jeb.098665

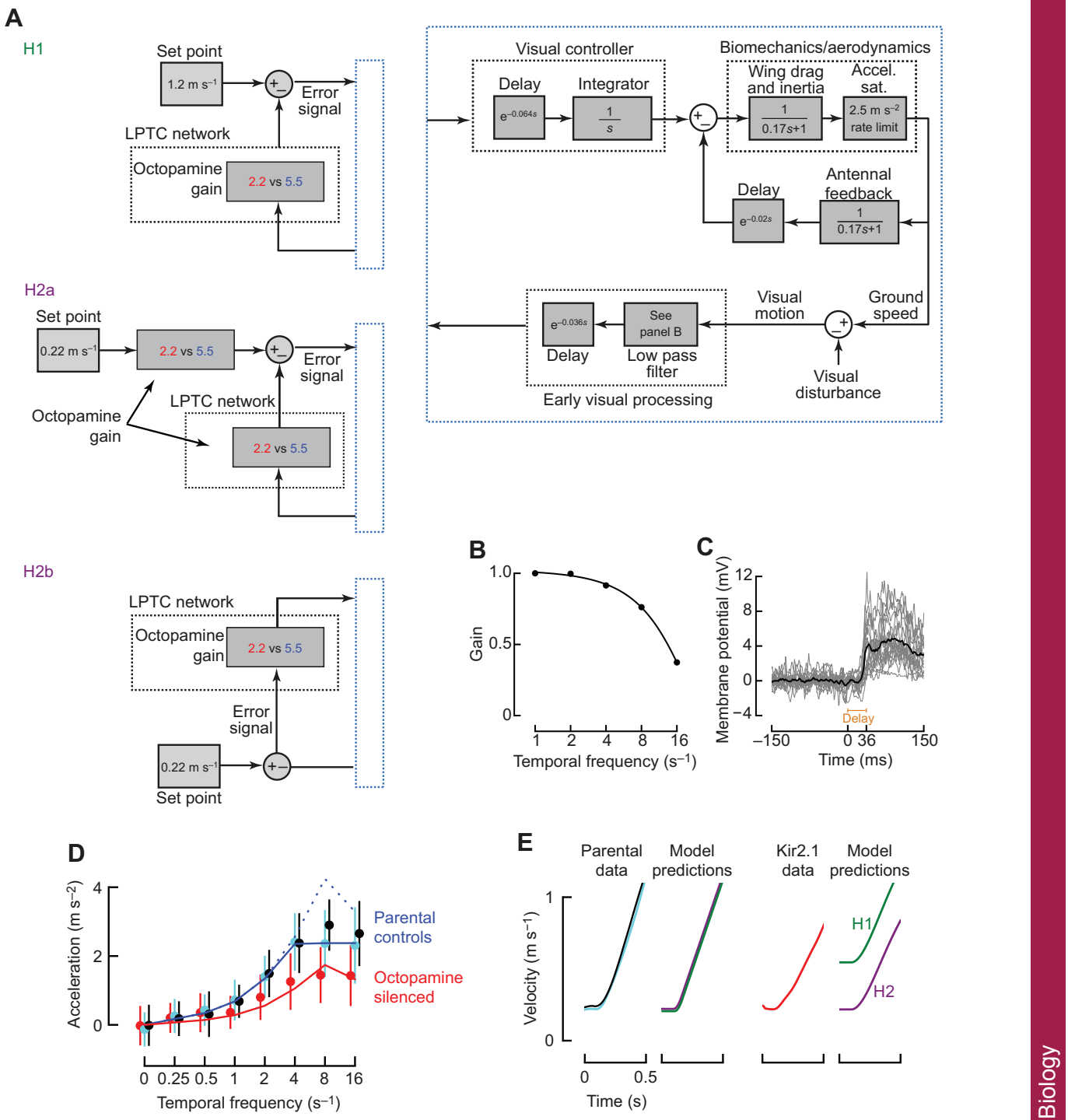

Fig. 4. Preferred visual motion set point is either modulated by changes in gain identical to those applied in the lobula plate tangential cell (LPTC) network (H2a), or the set point enters the visual sensory-motor cascade upstream of the LPTC network (H2b). (A) Block diagram showing the models under consideration. (B) Gain versus temporal frequency curve used for the low pass filter in the visual sensory system of our model. The data points are drawn from the temporal frequency tuning curve given in fig. 1D in Suver et al. (Suver et al., 2012), which summarizes the responses of electrophysiological recordings of vertical system (VS) cells in response to vertical motion. The original data were scaled such that the gain at a temporal frequency of 1 Hz is 1. The line shows a third-order polynomial fit. Note that this results in a transfer function defined in the linear temporal frequency domain, rather than the oscillatory temporal frequency domain. In order to implement this type of filter in our control model, we calculate the gain based on the linear temporal frequency of the stimulus. (C) Baseline subtracted membrane potential of VS cells in response to a downward 8 Hz visual motion stimulus during flight; data repeated, and magnified, from Suver et al. (Suver et al., 2012). The gray traces show the mean responses each of 19 individual flies, and the bold trace shows the group mean. (D) Model predictions compared with our results from Fig. 3E. The solid blue line shows the model prediction for the parental controls (gain=5.5) with the biomechanical saturation, whereas the dotted blue line shows the prediction without saturation. The solid red line shows the model prediction for the flies with inactivated octopamine neurons (gain=2.2). Note that the models H1, H2a and H2b all give identical acceleration responses. (E) Model predictions (color coded consistently with A) compared with mean velocity versus time responses for parental controls (left) and flies with inactivated octopamine neurons (right). The data traces are repeated from Fig. 3A. Note that H2 is a better fit.

The Journal of Experimental Biology (2014) doi:10.1242/jeb.098665

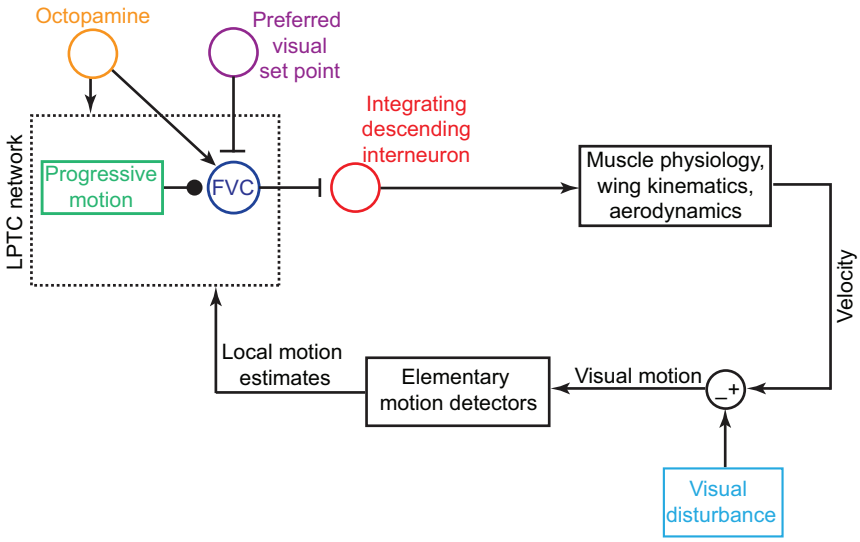

Fig. 5. Neural circuit summarizing the block diagram for H2b(i) from Fig. 1 in the context of a fly's hypothetical neuroanatomy. The simplest possible implementation is that a neuron within the LPTC network acts as a forward velocity controller (FVC) neuron, which either receives a signed translatory motion input or calculates it itself, and subtracts the preferred visual set point. The output of this cell is then modulated by octopamine. The FVC cell projects to descending interneurons, where the signal is integrated before activating motor-neurons in the thoracic ganglion. Octopamine also plays a role in modulation of other neurons throughout the LPTC network, such as the VS cells (Suver et al., 2012); this modulation is indicated by the smaller arrow.

two gain blocks in H2a would result in a shift in baseline flight speed. This could explain the slight increase in baseline flight speed we observed. However, time-dependent changes in the activity of octopamine neurons would result in unpredictable oscillations in flight speed (as illustrated in Fig. 1, H2a, blue trace). In H2b, in contrast, time-dependent changes in octopamine would serve to change the dynamics of the flies' response, rather than their steady-state activity (Fig. 1, H2b, blue trace). Given these potentially detrimental effects, we suspect that the H2a is less likely than the H2b model, although there is currently insufficient data to distinguish between them with certainty. To do so would require monitoring the time course of changes in the spatial distribution of octopamine throughout the brain during closed loop behavior.

For H2b, we present two mathematically identical architectures (see Fig. 1): (1) gain modulation could occur before the feedback control circuit (e.g. in the visual system), and (2) gain modulation could occur after the feedback control circuit (e.g. in the motor system). These architectures are mathematically identical (in a linear system, such as our model) because of the commutative property of sequential blocks within a block diagram. In other words, H2b does not explicitly predict where the gain modulation takes place, it only asserts that the gain modulation must come after the point where sensory feedback and a set point are compared. Previous electrophysiological recordings, however, have established that gain modulation occurs within the LPTC network (Jung et al., 2011; Longden and Krapp, 2009; Longden and Krapp, 2010; Suver et al., 2012), suggesting that the preferred flight speed set point may enter the visual sensory-motor cascade upstream of the LPTC network [H2b(i)], which implies that the functional role of the network is not limited to constructing matched filters for self-motion, but also involves integration of additional internal and external signals. The LPTC neurons synapse directly onto descending interneurons that project to neck, leg and wing motor centers in the thoracic ganglia (Gronenberg and Strausfeld, 1990; Strausfeld and Bassemir, 1985; Strausfeld and Seyan, 1985). Thus, the major output elements of the LPTC network are only one to two synapses away from motor neurons, and it is reasonable to propose that control signals, such as those determining the forward velocity set point, might enter the sensory-motor path within the LPTC network rather than downstream from it.

Octopamine neurons, however, project throughout the brain (Fig. 2B), resulting in a vastly more complex network of modulation than accounted for by either the H1 or H2 models. In addition to its role in the LPTC network, octopamine has been implicated in modulation of contrast sensitivity and motion adaptation in visual processing presynaptic to the LPTC network, presumably within the elementary motion detection circuits (de Haan et al., 2012). Because contrast has been shown to influence baseline flight speed (Straw et al., 2011), octopamine could have an indirect influence on a flies' preferred visual set point, which could also explain the slight increase in baseline flight speed that we observed.

In summary, our data provide strong evidence in favor of H2 over H1 (Fig. 4D,E); however, distinguishing between H2a and H2b is beyond the capability of current techniques. Because H2a could cause unpredictable oscillations in the flies' velocity (as illustrated in Fig. 1, H2a, blue trace), we believe H2b to be a more likely model. The key architectural implication of H2b is that gain modulation occurs after the comparison between a preferred set point and sensory feedback. Because gain modulation is known to occur within the LPTC network, which likely plays a role in the groundspeed regulator of the fly, the H2b model implies that the preferred set point must enter the visual-motor pathway upstream of the LPTC [H2b(i)].

To place our H2b(i) model within in the context of the flies' known neural architecture, we constructed a simple putative neural circuit (Fig. 5). The key conclusion from our experimental and modeling results is that the octopamine gain is likely applied after the flies' estimate of translational motion is compared with its preferred visual set point. We hypothesize that this comparison, and the subsequent octopaminergic gain modulation, is mediated by a putative neuron within the lobula plate that we call the forward velocity controller (FVC). The functions of the FVC could conceivably be performed by previously characterized LPTC cells. Alternatively, the FVC may represent a neuron (or sequence of neurons) that has not yet been identified. Previous studies suggest that the flies' preferred visual set point might be a function of visual cues such as total luminance, contrast and distance to objects, as well as olfactory cues (Tammero and Dickinson, 2002; Straw et al, 2011; van Breugel and Dickinson, 2014). Thus, future electrophysiological studies should investigate the influence of such sensory cues on the response properties of visual interneurons within the LPTC network. However, examining the effect of such cues on the visual set point will prove challenging. To our knowledge, no researcher has succeeded in implementing a closed-loop protocol for

forward translational control within a tethered flight arena. In our free-flight experiments, the flies were inherently always in closed loop, guaranteeing reasonably natural behavioral responses.

MATERIALS AND METHODS

Animals

Experiments were performed on 2- to 3-day-old fruit flies, *Drosophila melanogaster* Meigen, using the following transgenic constructs in a w[+] Canton-S genetic background: *Tdc2-Gal4* (FBst0009313) and *UAS-Kir2.1-EGFP* (FBti0017552). In the text, the parental controls are always referenced in the following order: *UAS-Kir2.1*, *Tdc2-Gal4*. Flies were deprived of food, but not water, for 6–8 h prior to the start of the experiment in order to motivate flight. For each experimental trial, we introduced a group of 12 flies to the corner of the arena within a small test tube. The flies were then free to move throughout the flight arena for a period of 12–18 h, during which time data were collected automatically. With the exception of the experiment shown in Fig. 3C, all experiments were performed with female flies.

Flight arena

We performed all experiments in a 1.5×0.3×0.3 m working section of a wind tunnel (Fig. 1) that has been described previously (Budick and Dickinson, 2006; Maimon et al., 2008; Straw et al., 2010; van Breugel and Dickinson, 2012). In these experiments, the wind tunnel was switched off, so that the internal air was still. Therefore, we refer to the arena as a 'tunnel' throughout the paper. On the two long walls and floor of the arena we projected a sine grating perpendicular to the length of the tunnel with a constant linear spatial frequency of 4.2 m^{-1} using a Lightspeed Designs DepthQ projector (Oregon City, OR, USA) with the color wheel removed (120 Hz update rate, 360 Hz frame rate, mean luminance 50 cd m^{-2}). The spatial frequency was chosen because it lies within the range of maximum response for similar visuomotor behaviors in a similar arena (Fry et al., 2009; Straw et al., 2010). We generated the sine grating, and controlled its temporal frequency, using the VisionEgg open-source image-rendering software (Straw, 2008).

We tracked the 3D position of individual flies within the chamber using a real-time tracking system that is described in detail elsewhere (Straw et al., 2011). The 10-camera (Basler Ace 640-100 gm, Basler, Exton, PA, USA) system generated an estimate of the fly's position at 100 frames s^{-1} with a median latency of 39 ms. For the purposes of tracking, the arena was backlit with an array of near-infrared (850 nm) LEDs. The cameras were equipped with long-pass filters (Hoya R-72) so that the camera images were not contaminated by the pattern that was displayed in visible wavelengths.

Experiment protocol

To automate the data collection, we used a position- and velocity-dependent trigger near both ends of the tunnel. When a fly passed through either trigger volume while flying towards the opposite end of the tunnel, the visual display of sine gratings began to move randomly at one of eight specified temporal frequencies (0–16 Hz), in the same direction as the fly's initial motion. The stimulus continued to move for 12 s, which was more than sufficient time for the fly to reach the opposite end of the tunnel. We restricted our analysis to the first 0.5 s of these trajectories. After each visual presentation there was a refractory period of 25 s during which time the trigger remained off regardless of the fly's behavior.

Trajectory reconstruction and analysis

All analyses of flight trajectories were performed using custom software written in Python using the open-source software packages Scipy and MatPlotLib, as well as MATLAB. Each trajectory was treated as an independent sample, as the tracking software was not able to maintain fly identities over the extended period of our experiments. Therefore, we could not test whether individual flies behaved consistently differently from other flies. We tested 24 individual flies for each of the parental controls and 108 *Tdc2-Gal4*/*UAS-Kir2.1-EGFP* flies, resulting in 42–106 trajectories for each temporal frequency and each of the three genetic lines. Trajectories that came within 5 cm of the tunnel ceiling, or turned around part way through the trial, were left out of our analysis. Each trajectory was smoothed to remove digitization errors, and to estimate velocity and acceleration, using a simple forward/reverse, non-causal Kalman filter. We measured a 19±1 ms delay between the computer generating the visual stimulus and the projector (Fuller et al., 2014). Adjustments were made to the trajectories to align them with the true estimated timing of the stimulus *post facto*. Means and standard deviations of the accelerations in response to the visual stimulus were calculated by averaging the Kalman estimates of acceleration for the time range of 200–400 ms after the onset of visual motion. In Fig. 3A–E, we report the forward velocity component in the direction of the visual motion. In Fig. 3F, we report the horizontal flight speed, which includes both the component in the direction of visual motion and the component perpendicular to visual motion.

All statistical comparisons were performed with the two-tailed Mann–Whitney *U* test. Statistically significant differences at the P=0.001 level were calculated using the Bonferroni method for multiple hypothesis testing (Shaffer, 1995). We used open-source Python software for computing the statistically homogeneous groups, which is described in detail elsewhere (Robie et al., 2010; Dickinson, 2010). This software is freely available (http://astraw.github.com/pairs2groups/).

Immunohistochemistry and imaging

We dissected brains in 4% paraformaldehyde in PBS and fixed them for a total of 30 min. We then incubated them overnight at 4°C in a primary antibody solution containing 5% normal goat serum in PBS-Tx, mouse anti-nc82 (1:10, DSHB) and rabbit anti-GFP (1:1000, Invitrogen). Brains were then incubated for 2 h at room temperature in a secondary antibody solution containing 5% normal goat serum in PBS-Tx, goat anti-mouse Alexa Fluor 633 (1:250, Invitrogen) and goat anti-rabbit Alexa Fluor 488 (1:250, Invitrogen). We then mounted the brains in Vectashield and imaged them on a Leica SP5 II confocal microscope under 20× magnification and scanned them at 1 µm section intervals. We adjusted intensity and contrast for single channels for the entire image using ImageJ 1.46r.

Acknowledgements

The authors thank Anne Sustar and Ainul Huda for helping to create the necessary genetic constructs, and running experiments, as well as Dr Bettina Schnell and Dr Eatai Roth for providing valuable feedback on the manuscript.

Competing interests

The authors declare no competing financial interests.

Author contributions

The initial idea for these experiments came from work by M.P.S., who also provided the fly lines and performed confocal imaging. All authors worked together to design the experiments. F.v.B. performed the experiments, analysis, modelling and wrote the first draft of the paper. All authors contributed to the interpretation of results and revision of the manuscript.

Funding

Funding for this research was provided by The Hertz Foundation Graduate Research Fellowship (F.v.B.); the National Science Foundation Graduate Research Fellowship (F.v.B.); the Air Force Office of Scientific Research FA9550-10-1-0368 (M.H.D.); and the Paul G. Allen Family Foundation Distinguished Investigator Award (M.H.D.)

References

Andermann, M. L., Kerlin, A. M., Roumis, D. K., Glickfeld, L. L. and Reid, R. C. (2011). Functional specialization of mouse higher visual cortical areas. *Neuron* **72**, 1025-1039.

Borst, A., Haag, J. and Reiff, D. F. (2010). Fly motion vision. *Annu. Rev. Neurosci.* **33**, 49-70.

Brinkworth, R. S. A. and O'Carroll, D. C. (2009). Robust models for optic flow coding in natural scenes inspired by insect biology. *PLOS Comput. Biol.* **5**, e1000555.

Budick, S. A. and Dickinson, M. H. (2006). Free-flight responses of *Drosophila melanogaster* to attractive odors. *J. Exp. Biol.* **209**, 3001-3017.

Busch, S., Selcho, M., Ito, K. and Tanimoto, H. (2009). A map of octopaminergic neurons in the *Drosophila* brain. *J. Comp. Neurol.* **513**, 643-667.

Chiappe, M. E., Seelig, J. D., Reiser, M. B. and Jayaraman, V. (2010). Walking modulates speed sensitivity in *Drosophila* motion vision. *Curr. Biol.* **20**, 1470-1475.

David, C. T. (1982). Compensation for height in the control of groundspeed by *Drosophila* in a new, 'Barber's Pole' wind tunnel. *J. Comp. Physiol.* **147**, 485-493.

de Haan, R., Lee, Y.-J. and Nordström, K. (2012). Octopaminergic modulation of contrast sensitivity. *Front. Integr. Neurosci.* **6**, 55.
Egelhaaf, M., Borst, A. and Reichardt, W. (1989). Computational structure of a biological motion-detection system as revealed by local detector analysis in the fly's nervous system. *J. Opt. Soc. Am. A* **6**, 1070-1087.
Fry, S. N., Rohrseitz, N., Straw, A. D. and Dickinson, M. H. (2009). Visual control of flight speed in *Drosophila melanogaster*. *J. Exp. Biol.* **212**, 1120-1130.
Fuller, S. B., Straw, A. D., Peek, M. Y., Murray, R. M., and Dickinson, M. H. (2014). Flying *Drosophila* stabilize their vision-based velocity controller by sensing wind with their antennae. *Proc. Natl. Acad. Sci. USA* (in press).
Geiger, G. and Nässel, D. R. (1981). Visual orientation behaviour of flies after selective laser beam ablation of interneurones. *Nature* **293**, 398-399.
Gronenberg, W. and Strausfeld, N. J. (1990). Descending neurons supplying the neck and flight motor of Diptera: physiological and anatomical characteristics. *J. Comp. Neurol.* **302**, 973-991.
Haikala, V., Joesch, M., Borst, A. and Mauss, A. S. (2013). Optogenetic control of fly optomotor responses. *J. Neurosci.* **33**, 13927-13934.
Hassenstein, B. and Reichardt, W. (1956). Systemtheoretische analyse der zeit-, reihenfolgen- und vorzeichenauswertung bei der bewegungsperzeption des russelkafers chlorophanus. *Z. Naturforsch. B* **11**, 513-524.
Hausen, K. and Wehrhahn, C. (1983). Microsurgical lesion of horizontal cells changes optomotor yaw responses in the blowfly *Calliphora erythrocephala*. *Proc. R. Soc. B* **219**, 211-216.
Heisenberg, M., Wonneberger, R. and Wolf, R. (1978). Optomotor-blind H31 – a *Drosophila* mutant of the lobula plate giant neurons. *J. Comp. Physiol.* **124**, 287-296.
Johns, D. C., Marx, R., Mains, R. E., O'Rourke, B. and Marbán, E. (1999). Inducible genetic suppression of neuronal excitability. *J. Neurosci.* **19**, 1691-1697.
Jung, S. N., Borst, A. and Haag, J. (2011). Flight activity alters velocity tuning of fly motion-sensitive neurons. *J. Neurosci.* **31**, 9231-9237.
Karmeier, K., van Hateren, J. H., Kern, R. and Egelhaaf, M. (2006). Encoding of naturalistic optic flow by a population of blowfly motion-sensitive neurons. *J. Neurophysiol.* **96**, 1602-1614.
Kern, R., van Hateren, J. H., Michaelis, C., Lindemann, J. P. and Egelhaaf, M. (2005). Function of a fly motion-sensitive neuron matches eye movements during free flight. *PLoS Biol.* **3**, e171.
Krapp, H. G. and Hengstenberg, R. (1996). Estimation of self-motion by optic flow processing in single visual interneurons. *Nature* **384**, 463-466.
Lagarias, J. C., Reeds, J. A., Wright, M. H. and Wright, P. E. (1998). Convergence properties of the Nelder–Mead simplex method in low dimensions. *SIAM J. Optimization* **9**, 112-147.
Longden, K. D. and Krapp, H. G. (2009). State-dependent performance of optic-flow processing interneurons. *J. Neurophysiol.* **102**, 3606-3618.
Longden, K. D. and Krapp, H. G. (2010). Octopaminergic modulation of temporal frequency coding in an identified optic flow-processing interneuron. *Front. Syst. Neurosci.* **4**, 153.
Maimon, G., Straw, A. D. and Dickinson, M. H. (2008). A simple vision-based algorithm for decision making in flying *Drosophila*. *Curr. Biol.* **18**, 464-470.
Maimon, G., Straw, A. D. and Dickinson, M. H. (2010). Active flight increases the gain of visual motion processing in *Drosophila*. *Nat. Neurosci.* **13**, 393-399.
Marder, E. and Bucher, D. (2007). Understanding circuit dynamics using the stomatogastric nervous system of lobsters and crabs. *Annu. Rev. Physiol.* **69**, 291-316.
Medici, V. and Fry, S. N. (2012). Embodied linearity of speed control in *Drosophila melanogaster*. *J. R. Soc. Interface* **9**, 3260-3267.
Monastirioti, M., Linn, C. E., Jr and White, K. (1996). Characterization of *Drosophila* tyramine beta-hydroxylase gene and isolation of mutant flies lacking octopamine. *J. Neurosci.* **16**, 3900-3911.
Moran, J. and Desimone, R. (1985). Selective attention gates visual processing in the extrastriate cortex. *Science* **229**, 782-784.
Niell, C. M. and Stryker, M. P. (2010). Modulation of visual responses by behavioral state in mouse visual cortex. *Neuron* **65**, 472-479.
Ofstad, T. A., Zuker, C. S. and Reiser, M. B. (2011). Visual place learning in *Drosophila melanogaster*. *Nature* **474**, 204-207.
Orchard, I., Ramirez, J.-M. and Lange, A. B. (1993). A multifunctional role for octopamine in locust flight. *Annu. Rev. Entomol.* **38**, 227-249.
Robie, A. A., Straw, A. D. and Dickinson, M. H. (2010). Object preference by walking fruit flies, *Drosophila melanogaster*, is mediated by vision and graviperception. *J. Exp. Biol.* **213**, 2494-2506.
Rohrseitz, N. and Fry, S. N. (2011). Behavioural system identification of visual flight speed control in *Drosophila melanogaster*. *J. R. Soc. Interface* **8**, 171-185.
Shaffer, J. P. (1995). Multiple hypothesis testing. *Annu. Rev. Psychol.* **46**, 561-584.
Simpson, J. H. (2009). Mapping and manipulating neural circuits in the fly brain. *Adv. Genet.* **65**, 79-143.
Strausfeld, N. J. and Bassemir, U. K. (1985). Lobula plate and ocellar interneurons converge onto a cluster of descending neurons leading to neck and leg motor neuropil in *Calliphora erythrocephala*. *Cell Tissue Res.* **240**, 617-640.
Strausfeld, N. J. and Seyan, H. S. (1985). Convergence of visual, haltere, and prosternal inputs at neck motor neurons of *Calliphora erythrocephala*. *Cell Tissue Res.* **240**, 601-615.
Straw, A. D. (2008). Vision egg: an open-source library for realtime visual stimulus generation. *Front. Neuroinform.* **2**, 4.
Straw, A. D., Lee, S. and Dickinson, M. H. (2010). Visual control of altitude in flying *Drosophila*. *Curr. Biol.* **20**, 1550-1556.
Straw, A. D., Branson, K., Neumann, T. R. and Dickinson, M. H. (2011). Multi-camera real-time three-dimensional tracking of multiple flying animals. *J. R. Soc. Interface* **8**, 395-409.
Suver, M. P., Mamiya, A. and Dickinson, M. H. (2012). Octopamine neurons mediate flight-induced modulation of visual processing in *Drosophila*. *Curr. Biol.* **22**, 2294-2302.
Tammero, L. and Dickinson, M. H. (2002). The influence of visual landscape on the free flight behavior of the fruit fly *Drosophila melanogaster*. *J. Exp. Biol.* **205**, 327-343.
Treue, S. and Maunsell, J. H. R. (1996). Attentional modulation of visual motion processing in cortical areas MT and MST. *Nature* **382**, 539-541.
van Breugel, F. and Dickinson, M. H. (2012). The visual control of landing and obstacle avoidance in the fruit fly *Drosophila melanogaster*. *J. Exp. Biol.* **215**, 1783-1798.
van Breugel, F. and Dickinson, M. H. (2014). Plume-tracking behavior of flying *Drosophila* emerges from a set of distinct sensory-motor reflexes. *Current Biology* **24**, 274-286.
Venken, K. J. T., Simpson, J. H. and Bellen, H. J. (2011). Genetic manipulation of genes and cells in the nervous system of the fruit fly. *Neuron* **72**, 202-230.